

Development and characterization of a secondary RF plasma-assisted closed-field dual magnetron sputtering system for optical coatings on large-area substrates

This article has been downloaded from IOPscience. Please scroll down to see the full text article.

2010 Plasma Sources Sci. Technol. 19 025011

(<http://iopscience.iop.org/0963-0252/19/2/025011>)

View [the table of contents for this issue](#), or go to the [journal homepage](#) for more

Download details:

IP Address: 128.174.163.99

The article was downloaded on 28/07/2011 at 18:44

Please note that [terms and conditions apply](#).

Development and characterization of a secondary RF plasma-assisted closed-field dual magnetron sputtering system for optical coatings on large-area substrates

R Raju¹, L Meng¹, R Flauta¹, H Shin¹, M J Neumann, T A Dockstader²
and D N Ruzic¹

¹ Center for Plasma Material Interactions, University of Illinois at Urbana-Champaign, Urbana, IL- 61801, USA

² Kurt J Lesker Company, Clairton, PA, USA

E-mail: rflauta@illinois.edu

Received 28 July 2009, in final form 4 January 2010

Published 8 March 2010

Online at stacks.iop.org/PSST/19/025011

Abstract

An RF-assisted closed-field dual magnetron sputtering system was developed to characterize the plasma and the ionization fraction of sputtered material to provide a suitable system for depositing optical thin films on large-area substrates at low temperatures (<130 °C). The 'prototype' system consists of dual 76 mm dc magnetrons operated at both balanced and unbalanced (closed-field) configurations with an RF coil to initiate a secondary plasma. The RF plasma assistance enhanced the electron density to one order of magnitude higher, increased the deposition rate and effectively enhanced the ionization fraction of the sputtered flux to above 80% as measured from the quartz crystal microbalance combined with electrostatic filters. Based on the prototype system, a large-scale RF-assisted system using two 9 × 46 cm linear magnetron cathodes was also developed and evaluated. Both systems were also tested for reactive deposition of indium tin oxide on both small-scale and large-area polyethylene terephthalate substrates with the actual substrate surface temperature monitored to be <130 °C. From both the evaluation results of the plasma characterization and deposition performance, the prototype and the large linear magnetron system were found to be suitable for reactive thin film deposition of compound targets that can be extended to various types of optical coatings.

(Some figures in this article are in colour only in the electronic version)

1. Introduction

Magnetron sputtering has been widely used in the manufacturing of industrial coatings. It offers a flexible deposition process of thin films with high throughput and can be used for high-purity thin film fabrication in semiconductors or for large-area coatings of structural materials such as glass windows. One of the main advantages of magnetron sputtering over other competing physical vapor deposition techniques is the additional kinetic energy of the sputtered atoms resulting in a more adherent and better conformal coating coverage. This kinetic energy is also responsible for the formation of

many different compound thin films which can be deposited at much lower temperature, giving numerous advantages when deposition is done on temperature-sensitive substrates [1, 2].

One of the more recent developments in magnetron system is the use of dual magnetron sputtering system which can be operated in a 'balanced' mirrored configuration or an 'unbalanced' closed-field configuration [3]. The balanced configuration has a strong electron confinement which could give rise to repeated ionization of the process gas and thus a high sputtering rate. However, this confinement does not allow for a great deal of plasma to spread. In the unbalanced configuration some electrons are not confined but escape from

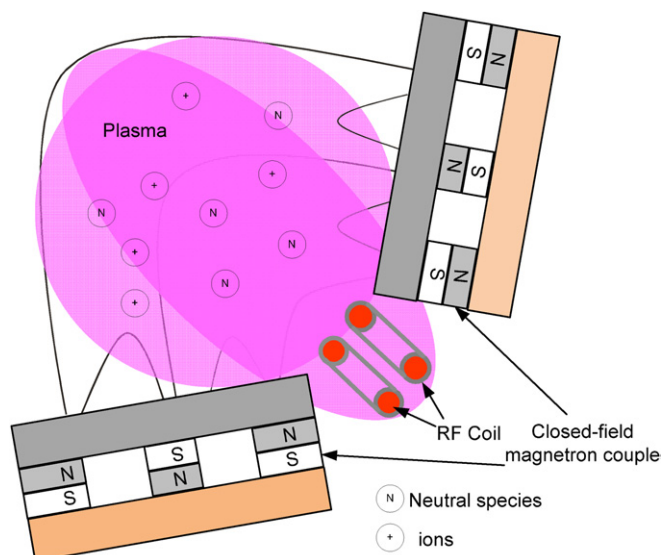


Figure 1. Schematic diagram of the closed-field (unbalanced) magnetron sputtering setup.

the target area. Two such unbalanced magnetrons neighboring each other with opposite polarities could form a ‘closed-field’ configuration, extending the plasma to the intervening region [4], as illustrated in figure 1. The addition of an RF coil between the magnetron pair further excites the plasma near the target, creating more ionization of the sputtered material. Combining the capabilities of the RF coil and the proper magnetic field configuration would result in denser plasma accelerated to the substrate region providing more flexibility in the sputtering process. Thus, an RF plasma-assisted closed-field dual magnetron sputtering system could be of considerable interest for many applications in thin film deposition.

To produce industry-standard transparent conducting oxide (TCO) and other compound thin films, the process usually involves deposition at relatively high substrate temperature in excess of 200 °C which increases further when annealing treatments are made on the films. For a TCO material such as indium tin oxide (ITO), it is desirable to grow the film onto flexible organic substrates for more fascinating applications. But the poor thermal endurance of the organic substrates demands a low substrate temperature during film growth, in addition to the desired deposition on a large area, high deposition rate, good uniformity and quality of the deposited materials. Different ways to add energy to the growing TCO films instead of heating the substrate have been investigated, such as the ion-assisted deposition [5, 6], ion beam sputtering [7, 8] and pulsed-laser deposition [9]. In these methods, the bombardment of energetic ions and atoms can improve the electrical and optical properties of the TCO film by transferring their kinetic energy to the surface adatoms and, in turn, modifying the surface morphology [10]. However, there is a concern that energetic ion radiation can cause damage to organic materials and result in degraded device performance [11]. Also these methods are typically limited to low-pressure operation with low deposition rate

and are difficult to adapt to large-area deposition. Plasma-assisted magnetron sputtering has also been reported to deposit TCO films at low temperature [12]. More ions are created by the secondary plasma assistance and potentially provide an efficient energy transfer to the growing films. It is of considerable interest to combine the plasma assistance with the closed-field dual magnetron as mentioned above. It is not only suitable for low temperature formation of good TCO films but also easy to achieve large-area capability (e.g. roll-to-roll) and high deposition rate.

In this paper, a new type of RF plasma-assisted magnetron sputtering system was developed. The dual magnetrons were arranged in a closed-field unbalanced configuration so that plasma is created in the intervening field rather than being confined near the target. An RF coil was added between the magnetrons to provide more plasma excitation in the bound region. 3D Langmuir probe diagnostics were performed to better understand the plasma properties of this configuration as well as the influences of RF assistance. Another important parameter of ionization fraction was measured using quartz crystal microbalance (QCM) with a gridded energy analyzer (GEA) to provide further insight into the benefits from this configuration. The system was tested to deposit thin film coatings of ITO and deposition was made at low substrate temperature using plastic substrates. Gentle ion bombardment due to the plasma sheath on the substrate strikes the growing film and deposits additional energy onto the film thus allowing lower temperature during deposition. The influence of RF power on the plasma density, plasma spatial distribution, ionization fraction of sputtered material and the influence of these parameters on some of the properties of the ITO film produced were explored.

2. Experiments

The schematic diagram of the prototype plasma-assisted closed-field magnetron sputtering system is shown in figure 2. It consists of two 76 mm cathodes placed at an angle of 150°, while the substrate holder is 64 mm away from the magnetron and was floating rather than biased. The magnetrons have been operated at both balanced and unbalanced (closed-field) configurations. To switch the magnetron from a balanced configuration to a ‘closed-field’ one, the strengths of the inner magnets were reduced (approximately from 4600 to 3500 G measured at the center of the magnet top surface) and the polarization of one magnetron was inverted such that a closed-magnetic field region is formed in the intervening space. In an Ar ambient gas, distinct shapes of the magnetron plasma were generated in the closed-field or unbalanced configuration compared with the balanced case where the plasmas originated from each magnetron were connected in the intervening area and extended to the substrate zone, as shown in figure 3. The vacuum system deployed both a turbo-pump and a cryo-pump to obtain a base pressure of 1.3×10^{-6} Pa. The samples were transferred via the loadlock chamber. An RF coil was designed, fabricated and added between the two magnetrons to provide more plasma excitation and create a higher ionization rate for the sputtered species. The RF coil has two loops and comes

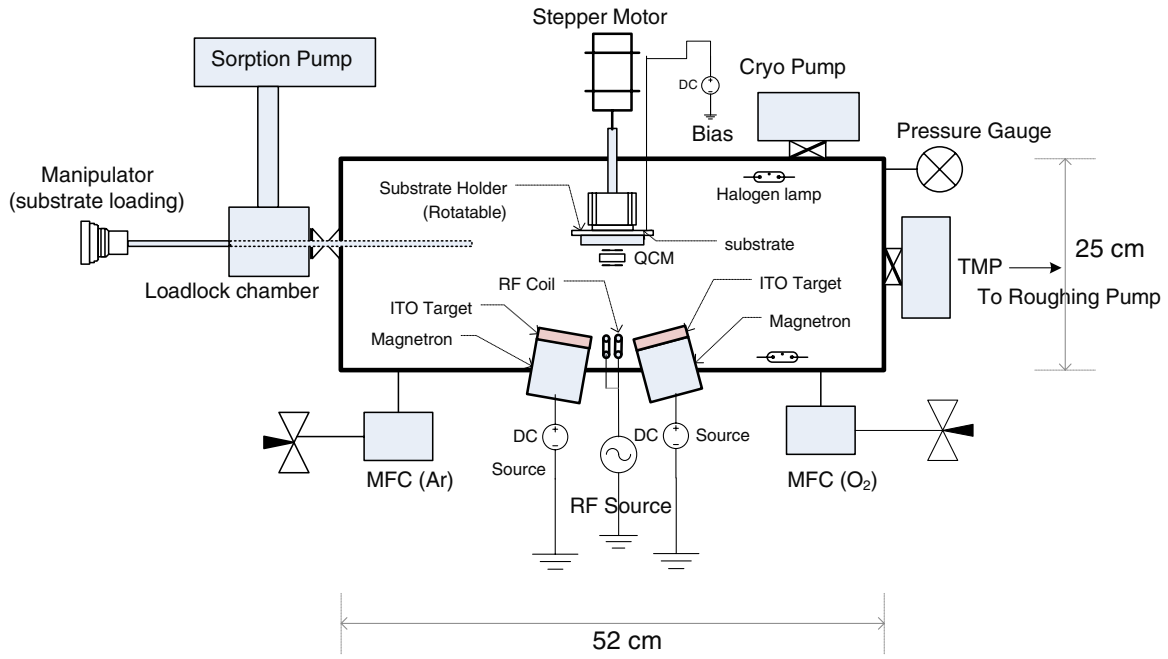


Figure 2. The prototype RF-assisted dual magnetron sputtering system.

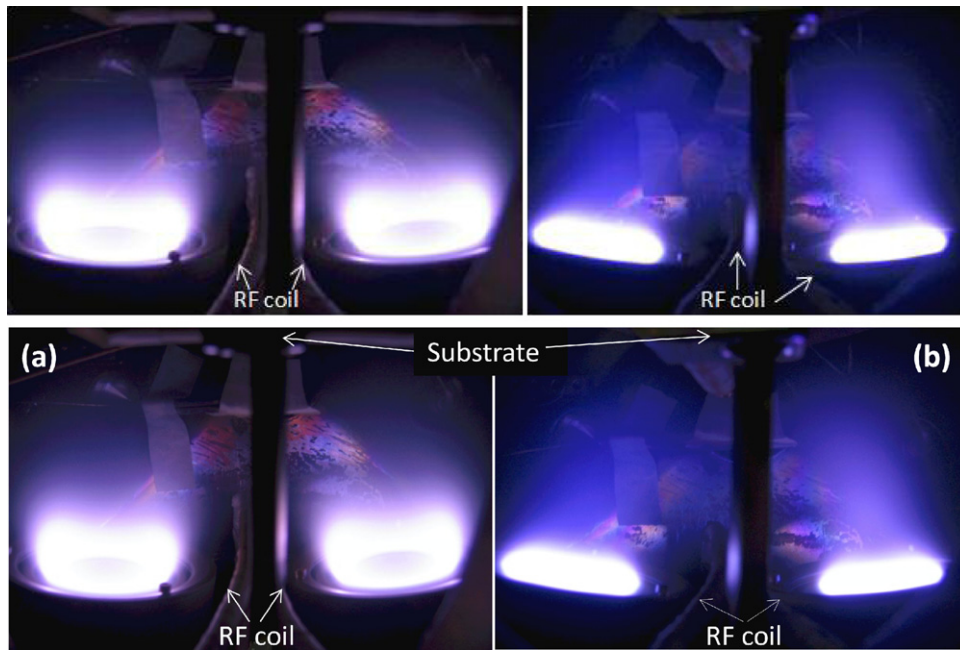


Figure 3. Cathode configurations: (a) balanced cathode configuration showing distinct ionization populations clustered at the magnetrons (b) unbalanced configuration where the coupling of the magnetic field leads to electron sharing and glow in an arch through the intended substrate deposition zone.

in and out of the page in figure 2. The normal to the plain of the antenna does not point at the substrate to allow it to fit between the magnetrons. The ITO target used in the thin film deposition is composed of 90% indium oxide (In_2O_3) and 10% tin oxide (SnO_2) by weight with purity of 99.99%. RF power during the ITO deposition was varied between 0 and 400 W.

An RF-compensated Langmuir probe was constructed to minimize the extraneous signals [13] and then mounted to a rotary-linear manipulator, as shown in figure 4(a). The probe tip was enabled to scan linearly from the magnetron

surface to the substrate and laterally from the midpoint of the two magnetrons to the farther end, 51 mm in the z direction and 89 mm in the r direction, respectively, as in figure 4(b). The electron temperature T_e and electron density n_e were obtained by analyzing the Langmuir probe $I-V$ traces according to the Laframboise method described by Ruzic [14]. The performance of the closed-field magnetron and the balanced magnetron configurations were first compared using the scanning Langmuir probe. The magnetrons were run at 50 mA of current and 0.67 Pa of Ar pressure without the RF

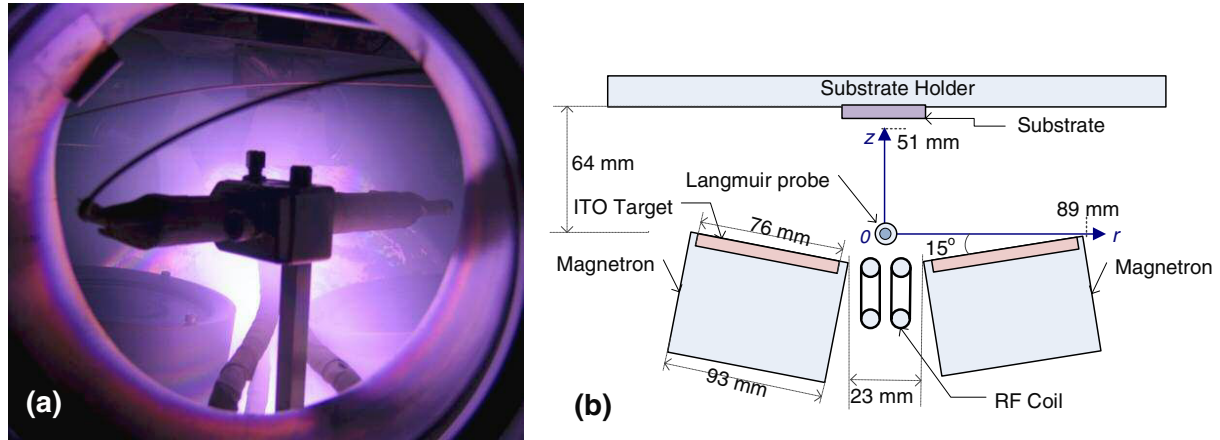


Figure 4. (a) The rotary-linear scanning RF-compensated Langmuir probe in the plasma. (b) The probe is able to move 51 mm in the z direction from the magnetron surface to the substrate and 89 mm in the r direction from the central coil to the edge of magnetron.

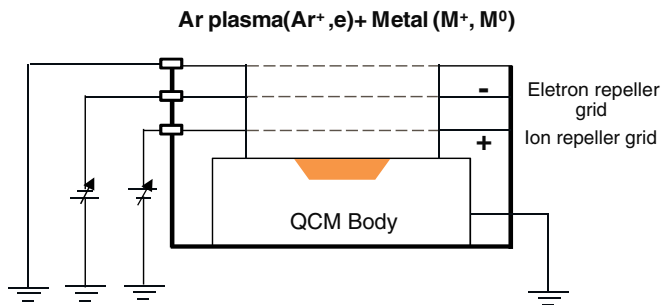


Figure 5. Schematic diagram of GEA and QCM.

assistance. The influence of the coupled RF plasma on the Ar sputtering plasma was subsequently investigated. Under a close-field magnetron configuration and the same settings of magnetron current and pressure as above, the RF power was increased from 0 to 200 W, when the spatial distribution of n_e and T_e was measured. It was observed in the process that the voltage on the dc magnetron decreased approximately from 230 to 170 V.

To estimate the ionization fraction of the sputtered metal flux, an electrostatic GEA was constructed and combined with a QCM. Figure 5 shows the schematic of the GEA located above the QCM. The top mesh grid was grounded to minimize the disturbance to the plasma while the middle grid (the electron repeller grid) was negatively biased around -15 V to reduce the electron penetration. The bottom grid, which acts as the ion repeller, was applied with an adjustable potential. When it was negatively biased (-10 V), the total flux of ions and neutrals ψ_{tot} was recorded by QCM [15]. When a positive bias was applied to the grid and gradually increased up to 50 V, only neutral flux ψ_N reached the QCM. The ion and neutral flux were further used to determine the ionization fraction of the metal flux. In both the balanced and closed-field unbalanced magnetron configurations, the effects of RF input power with respect to the ionization fraction ranged from 0 to 400 W with 50 mA of magnetron current and 0.67 Pa of gas pressure. And then without RF assistance, the pressure was adjusted from 0.13 to 2.67 Pa to study the effectiveness of the ionization.

The ITO film was then fabricated in the prototype RF-assisted close-field magnetron system. Both glass and polyethylene terephthalate (PET) were used as substrates which were fixed onto the sample holder. A temperature indicator was placed at the back side of the 0.127 mm thick PET sample to record the substrate temperature during the deposition process. To sputter out the ITO from the target, Ar + O₂ gas combinations were introduced inside the chamber controlled by mass flow controllers. The chamber pressure during deposition was kept at 6.7×10^{-1} Pa and the amount of O₂ in the gas mixture was at 2%. The operating magnetron current was 90 mA while RF power was varied between 0 and 400 W. With all these parameter settings the ITO was deposited for 45 min.

A four-point probe system was employed to measure the film resistivity combined with a surface profilometer to measure film thickness. Using an X-Rite 361T optical densitometer, the average light transmittance of the ITO film in the visible spectrum (340–650 nm) was determined from the measured optical density after correcting for the contributions of the uncoated substrate. X-ray photoelectron spectroscopy (XPS) was employed to determine the film stoichiometry. Since the surface geometry might affect the film properties significantly, atomic force microscopy (AFM) was used to characterize the film surface morphology in conjunction with the film properties.

After the demonstration and characterization on the above small-scale 76 mm magnetron system, the prototype system was adapted for large-area substrate deposition using a computer controlled deposition system. Two linear magnetrons of dimensions 9 cm \times 46 cm were held at an angle of approximately 90°. An RF coil was fabricated and modified for this larger cathode geometry and then fitted in the system as the RF plasma source. ITO deposition was then performed on a large-area PET plastic substrate (15 cm \times 38 cm) in accordance with the previous results. Magnetron current of 810 mA was initially chosen to achieve the same current density as in the 76 mm magnetron system. The chamber pressure was maintained at 0.67 Pa and the O₂ partial pressure was varied. Thin films of ITO were deposited for 10 min and

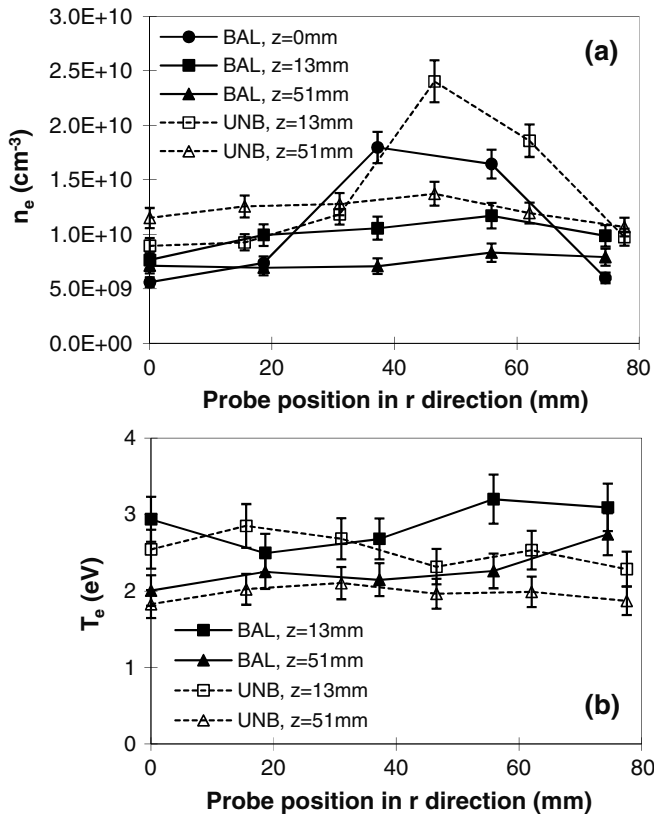


Figure 6. (a) Spatial distribution of n_e of the sputtering plasma in different magnetron configurations of balanced (BAL) and closed-field unbalanced (UNB). (b) The corresponding spatial distribution of T_e . The gas pressure and electrode current were at 0.67 Pa, 50 mA per cathode, respectively, without RF power. Measurements were performed near the magnetron ($z = 0, 13$ mm) and near the substrate ($z = 51$ mm).

then characterized for their optical transmittance and resistivity values.

3. Results and discussion

3.1. Langmuir probe diagnostics

Using the Langmuir probe, the spatial distribution of the sputtering plasma parameters such as the electron density n_e and the electron temperature T_e in different magnetron configurations was measured, as illustrated in figure 6. For the balanced magnetron, the distribution of the plasma showed a few distinct features. First, higher n_e was observed right around the center of the magnetron at $r = 37$ to $r = 56$ mm, as shown in the plane $z = 0$, where n_e increases from 5.6×10^9 cm⁻³ at $r = 0$ to a maximum of 1.8×10^{10} cm⁻³. Such a profile reflects the plasma confinement by magnetron which can also be observed directly from figure 3. Second, when the probe deviated away from the $z = 0$ plane, the n_e profile over r was immediately flattened out. Even in the plane of $z = 13$ mm, the peak could barely be seen. This implies that the plasma is intensively concentrated to the magnetron rather than being dispersed around, which is well in accordance with the magnetic field in balanced configuration. Third, when the probe was farther away from the target ($z = 51$ mm), n_e kept

decreasing to as low as 6.0×10^9 cm⁻³. When the magnetrons were switched to the closed-field unbalanced configuration, a different distribution scenario was observed. At the same plane $z = 13$ mm, an obvious peak point in the n_e profile still exists but is shifted to the right over the racetrack and is higher than that in the balanced configuration. Also at $z = 51$ mm, the n_e of the closed-field unbalanced configuration was evenly distributed at about 1.2×10^{10} cm⁻³, almost twice as high compared with the balanced configuration. It should be noted that the cathode voltage drops for these two setups were different even though the current per cathode was kept the same as 50 mA. The discharge voltage was 205 V for the balanced one compared with 250 V for the closed-field unbalanced case. This further confirms the fact that the plasma was more concentrated to the target in the balanced configuration so that the discharge voltage was lower in constant current mode. On the other hand, in a closed-field unbalanced configuration, the plasma was well diffused to the substrate, which could provide higher and more uniform metal flux to a large area of the substrate. Such profiles of n_e in the balanced and the closed-field unbalanced magnetron configurations well describe the shapes and conditions of the produced plasma as shown in figure 3.

The distribution of T_e was also characterized as shown in figure 6. The T_e was higher in the target region than near the substrate, likely because magnetic confinement prevents the high energy electrons from being easily lost to the wall. Also, T_e slightly decreased after switching from the balanced to the closed-field unbalanced configuration and became more uniform over the whole substrate at the farther position ($z = 51$ mm). Hence in terms of uniformity in T_e , having closed-field unbalanced magnetron may provide additional benefit for thin film deposition on a large substrate.

The influences of RF power on the sputtering plasma in the balanced and closed-field unbalanced magnetron are shown in figures 7 and 8, respectively. The profiles of the plasma distribution look similar for these two cases. Both the radial profiles of electron density at $z = 13$ mm and $z = 51$ mm were enhanced by one order of magnitude by applying 200 W of RF power. For the balanced one (figure 7), n_e was higher than in the closed-field unbalanced configuration (figure 8). This is understandable since the plasma in the closed-field unbalanced configuration was more diffusive due to the shape of the magnetic field. Also as mentioned in the experimental section, the strength of the inner magnets of the closed-field unbalanced magnetron was reduced which also weakened the plasma confinement. The n_e decreases smoothly over the r direction, which was dominated by the supplemental RF rather than by the magnetron sputtering plasma, while for T_e , no obvious effect of RF power was observed. In all, the RF plasma greatly enhances the electron density, which might further ionize the sputtered metal to facilitate the effective ITO deposition and energy transfer to the film.

3.2. Measurement of ionization fraction

The metal ionization fraction was estimated using the GEA combined with the QCM as described in the section 2 (see

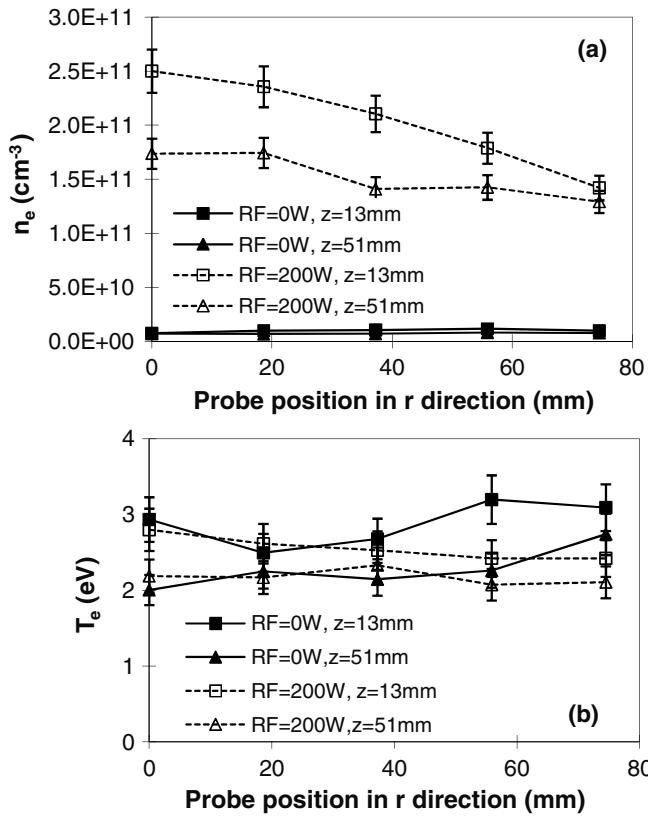


Figure 7. (a) Spatial profiles of n_e of plasma in the balanced configuration with and without supplemental RF assistance. (b) The corresponding T_e distribution. The gas pressure and electrode current were at 0.67 Pa, 50 mA per cathode, respectively. Measured at $z = 13$ mm and $z = 51$ mm.

figure 5). The influence of the magnetron configuration and RF power on the ionization fraction is shown in figure 9. In a balanced configuration, the ionization fraction increased from 50% to 85% as RF power increased from 0 to 200 W. After converting to the closed-field configuration, the ionization fraction was reduced, e.g. 5% without RF assistance. The plasma was more concentrated on the magnetron in the balanced mode which ionized the metal species sputtered out of the target more intensively and effectively. Also, as mentioned in section 2, the center magnets of the balanced magnetron pair are stronger, which also contributes to the higher ionization fraction in the balanced magnetron configuration. However this ratio could be compensated by the additional RF power, for example 200 W RF power increased the ionization fraction to 83%, almost the same as that of the balanced configuration. The incorporated RF secondary plasma provides denser electrons in the whole region. The ionization ratio was hence increased dramatically to a high value over 80%. It should be noted that our measurements were performed near the substrate plane rather than near the magnetron surface. A substantial fraction of neutral atoms will get scattered out of the plasma and lost to the chamber wall, while ions are much better confined in the plasma region to maintain the plasma charge neutrality, giving a higher ion fraction near the substrate as measured. With an increased ionization of the sputtered material, it is expected that the film deposition quality will be

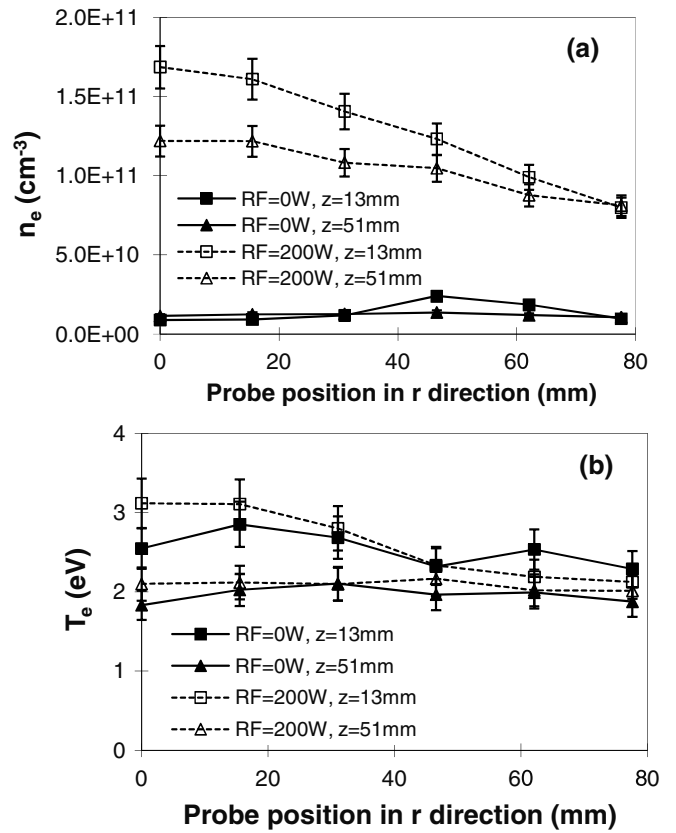


Figure 8. (a) Spatial distribution of n_e of the sputtering plasma in the closed-field (unbalanced) configuration with and without supplemental RF assistance. (b) The corresponding spatial distribution of T_e . The gas pressure and electrode current were at 0.67 Pa, 50 mA per cathode, respectively. Measured at $z = 13$ mm and $z = 51$ mm.

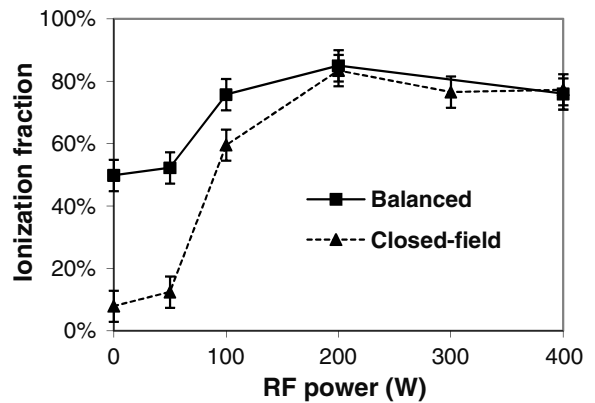


Figure 9. Ionization fraction measured in different magnetron configurations and at different RF powers. 0.67 Pa, 50 mA per cathode, RF power from 0 to 400 W.

enhanced by RF assistance both in the balanced and unbalanced configurations.

Further experiments were made to find the effect of gas pressure on the ionization fraction. No RF was introduced to identify the effect more obviously. As in figure 10, there is a maximum of ionization fraction at the middle-range pressure of around 1 Pa for both configurations. At lower pressure, the

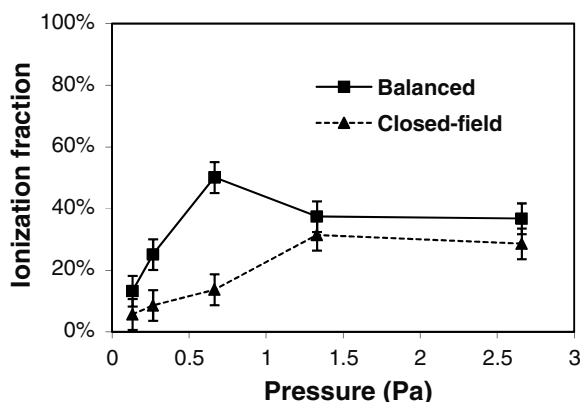


Figure 10. Effect of pressure on the ionization fraction, 0.13–2.67 Pa, 50 mA per cathode, No additional RF input.

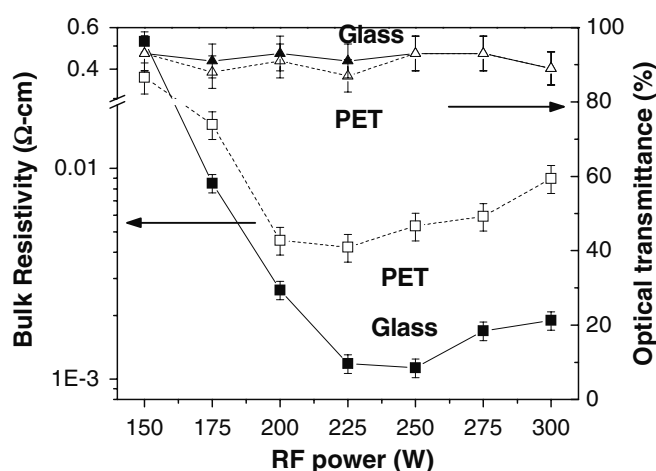


Figure 11. The bulk resistivity and average optical transmittance of the ITO films deposited with different additional RF powers. ITO was deposited at 0.67 Pa, 2% of O_2 in Ar, 90 mA cathode current while RF power was varied between 0 and 300 W.

mean free path of the particles is so large that the ionization of sputtered material is inefficient. At a higher pressure, too frequent scattering reduces the energy of electrons and thus the ionization cross section of atoms by electrons decreases.

3.3. ITO film deposition

Using the closed-field configuration, test depositions of ITO films were made on both glass and PET substrates, as described in section 2. Figure 11 shows the influence of additional RF power on the electric conductivity and average optical transmittance of the film in the visible spectrum. Here the bulk resistivity of the film was calculated as a product of the film thickness and the sheet resistance measured from the four-point probe. It turned out that at 150 W or below, barely no conductivity was identified on either the glass or PET samples. By adding more RF power, the film resistivity was significantly reduced and reached a minimum at around 225–250 W as $1.2 \times 10^{-3} \Omega \text{ cm}$ on the glass substrate, after which it began to increase again. The glass samples deposited at 150, 225 and 300 W of RF power were chosen for the further characterization and their electrical and optical properties

are compared in table 1. The lowest sheet resistance of $30 \Omega/\text{sq}$ was achieved at 225 W, and the bulk resistivity was calculated to be $1.2 \times 10^{-3} \Omega \text{ cm}$. Meanwhile, the optical transmittance of the film did not show large variation, basically above 91% for the glass sample and above 87% for PET. During the deposition process, the substrate temperature was monitored, which was shown to increase with a higher RF power (figure 12). For 225 W, the substrate temperature was well kept under 110°C , suitable for the organic substrate. The experiment results showed a clear trend that assisting RF power could increase the conductivity dramatically. Actually, the electrical properties here could be further improved, since our bulk resistivity is higher than $5 \times 10^{-1} \Omega \text{ cm}$ without RF assistance compared with a resistivity lower than $10^{-3} \Omega \text{ cm}$ reported using magnetron sputtering only [16]. Experiments are currently being performed, for example by optimizing the O_2 ratio and removing the diagnostic tools in the chamber. The results will be reported elsewhere.

It is known that in the conventional methods to prepare the ITO film, the deposition usually requires a sufficiently high substrate temperature to achieve good film properties [17]. The RF secondary plasma is proven as an effective approach to provide additional energy to the growing films. Due to the existence of RF plasma, more ions of $\text{Ar} + O_2$ and metal are generated. In fact, it has been verified that the ionization fraction increased at higher RF power. These ions after being accelerated by the plasma potential could directly deposit the energy to the substrate and thus promote the ITO growth. As in this experiment, the film deposited at 225 W was found thicker than at 150 and 300 W. Another possible reason for the improvement of film conductivity might be the more efficient creation of oxygen vacancies in the ITO film. It has been widely observed that oxygen partial pressure can significantly affect the ITO film resistivity [18–20]. It was found that even though the ITO evaporation source itself has stoichiometric oxygen content in the material, oxygen deficient films were obtained under no or low additional oxygen flux conditions exhibiting a high resistance and low optical transmittance. Additional oxygen was necessary to increase the oxygen ion beam flux and thus increase the oxygen incorporation into the oxygen-deficient ITO film which reduced the resistivity by compensating too high oxygen vacancies in the film. However, too high oxygen flow decreased oxygen vacancies in the film more than the required amount and resulted in an increase in the resistivity again [18]. In our set-up, even though the oxygen partial pressure was fixed, the oxygen ion flux could be increased by the additional RF plasma. It turned out that the RF power of 225 W generated the most appropriate oxygen ion flux, to get the lowest resistivity of the film.

The stoichiometry of the ITO film was further determined with the XPS, which showed consistent results for the ITO films deposited at different RF powers having almost identical atomic stoichiometry. High resolution XPS scan of the In3d5, Sn3d5 and O1s gives the atomic composition as 34.3%, 3.7% and 62.0%, respectively, which accorded well with the realistic ITO composition of 90% In_2O_3 and 10% SnO_2 by weight (with ITO stoichiometry of 35.6% : 3.6% : 60.7% for In : Sn : O).

The AFM images revealed that samples deposited at different RF powers exhibited distinct surface morphologies,

Table 1. Properties of the films deposited at 150, 225 and 300 W. Here the thickness was measured by profilometer.

RF power (W)	Cathode current (mA)	Substrate temperature (°C)	Thickness (nm)	Sheet resistance (Ω/sq)	Resistivity ($\Omega \text{ cm}$)	Transmittance (%)
150	90	66	334	16 500	5.5×10^{-1}	93
225	90	110	412	30	1.2×10^{-3}	91
300	90	127	346	57	2.0×10^{-3}	89

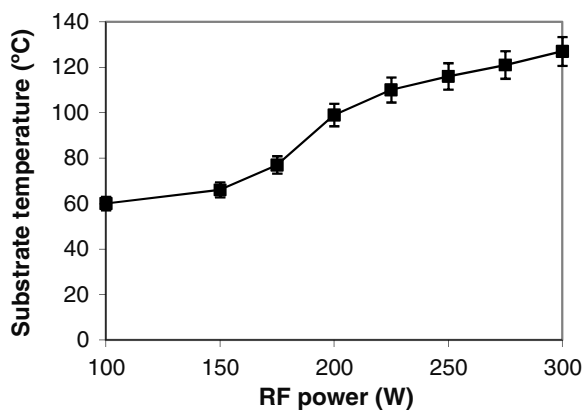


Figure 12. The substrate temperature at varied input RF powers.

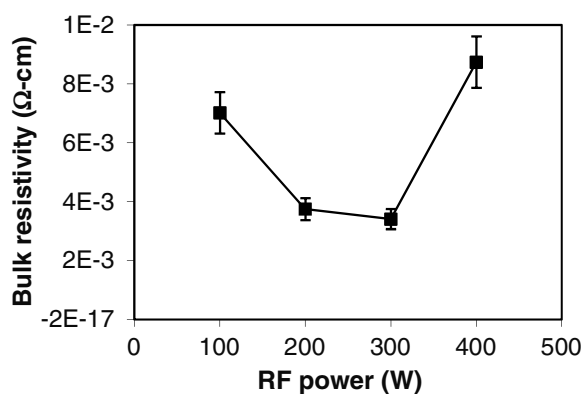


Figure 14. Influence of RF power on the resistivity of ITO film on PET substrate, at 0.8 A of cathode current, 0.67 Pa of Ar and base pressure of 2.7×10^{-3} Pa.

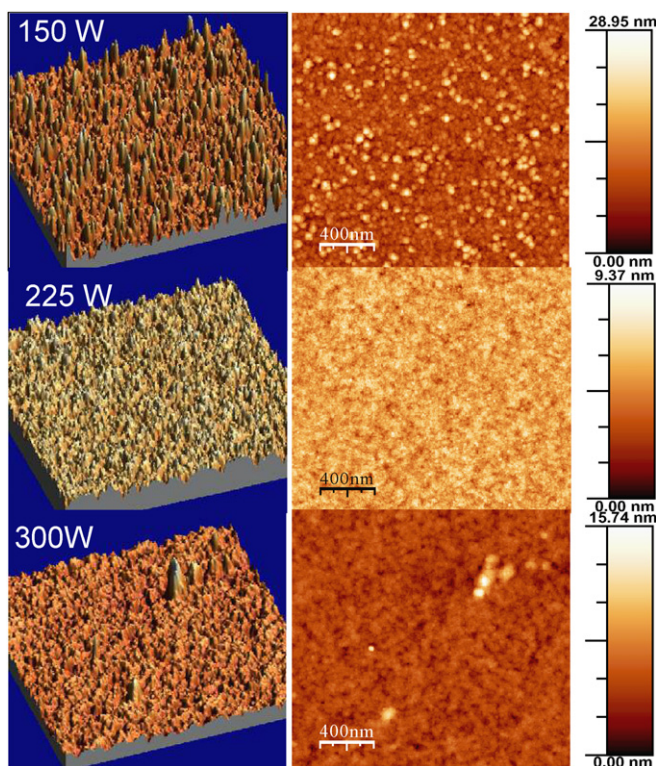


Figure 13. AFM scans of the films deposited at different RF power conditions.

as shown in figure 13. The sample at 150 W RF showed the roughest surface with an rms roughness of 3.3 nm with large grains on it. For 225 W, the rms roughness of surface was reduced to 0.9 nm and the grains were much finer. Even though Lee [21] has reported a surface roughness of IZO thin film as 0.7 nm using an ion-assisted deposition system,

attributing to the enhanced surface mobility of adatoms by ion bombardment, our result was still lower than the other typical values around 1–2.5 nm [6, 8]. The sample of 300 W revealed a similar surface morphology as with the 225 W sample, with an rms roughness of 1.1 nm. Thus, the flatness of the film surface was improved and the grain size became smaller with an increased RF power, which is important for the application in OLEDs or other opto-electronic devices.

It was reported that by increasing the deposition flux, the mobility of adatom or adsorbed molecules on the substrate surface could be reduced due to the supersaturation of adatoms. The mean free path of adatoms is reduced for nucleation, hence the size of formed particles is diminished and the surface becomes flat [22]. The promotion of RF on the oxygen ionization might also contribute to the smaller grain size at higher RF power. More oxygen is incorporated in the films on interstitial lattice sites, which hampers grain growth due to the formation of more grain boundaries, dynamic incorporation and segregation of oxygen during deposition [18, 23].

3.4. Deposition on large-area substrate

Using the 9 cm × 46 cm magnetron facility for large-area substrates, trial runs were made to be able to deposit films on PET. At a deposition time of 10 min varying the different plasma operating parameters, a film thickness range 250–400 nm was achieved. By operating at different RF powers, lower electrical resistivity values were observed as shown in figure 14. A bulk resistivity of $3.4 \times 10^{-3} \Omega \text{ cm}$ with the light transmittance of 90% was obtained on PET at 300 W RF (0.8 A cathode current, 0.67 Pa, 0% O₂/Ar, base pressure 2.7×10^{-3} Pa). A further increase to 400 W revealed an

abrupt increase in resistivity. Such a trend is similar to that in the small scale system. This change was attributed to the different energies transferred to the surface and to the oxygen incorporation during the film growth at different RF powers. The actual substrate surface temperature during the processes was monitored to be below 130 °C; thus deposition onto the plastic substrate at significant rates of 25–42 nm min⁻¹ while maintaining a substrate temperature below the PET substrate threshold has been demonstrated. In this case, by additional substrate cooling, which can be employed in the current set-up, a further reduction in the substrate surface temperature can be made.

By increasing the magnetron current to 1.6 A and adjusting the O₂ content to 0.5% in total gas, an ITO film of 520 nm was deposited at 300 W of RF assistance. The bulk resistivity was lowered down to $1.4 \times 10^{-3} \Omega \text{ cm}$ and the transmittance was 89%. The substrate temperature went up to 127 °C in the 10 min deposition process. However, in order to get a thickness of 150 nm to satisfy the industry requirement, only 3 min deposition time was required and under this condition, the temperature was kept at around 110 °C.

4. Conclusion

A coupled RF plasma source incorporated in a closed-field dual magnetron sputtering system was developed and its appropriate plasma parameters were characterized. Without RF assistance, the closed-field unbalanced magnetron configuration was observed to generate a higher-density and more uniform sputtering plasma above the substrate as compared with the balanced configuration. Additional RF source further enhanced the electron density to one order of magnitude higher, thus increasing the deposition rate. The presence of RF plasma also effectively increased the metal ionization fraction to above 80% based on the measurement using the QCM combined with electrostatic filters. Using ITO as a test film for deposition, ITO film was deposited on glass and plastic substrates in the closed-field configuration, the coupled RF plasma was shown to improve the film conductivity due to the higher energy transferred to the film and more oxygen incorporation in the ITO. A thin ITO film with resistivity of $1.2 \times 10^{-3} \Omega \text{ cm}$ and 91% of visible light transmittance was obtained at the 90 mA cathode current, 0.67 Pa, 2% of O₂ in Ar and 225 W RF, with the monitored substrate temperature at 110 °C. This condition was deemed significant since deposition at lower temperature, given the large-scale plasma parameter, is necessary for the process to be feasible for large volume production. AFM images also revealed that the surface roughness could also be improved by the RF assistance facilitating ITO film suitable for opto-electronic applications. The prototype has also been extended to larger rectangular magnetrons in a real flat panel display manufacturing system. The initial experiments obtained ITO films on a large-area plastic substrate, with a resistivity of $1.4 \times 10^{-3} \Omega \text{ cm}$ and an optical transmittance of while maintaining a substrate 89%. The system enables significant rates of 25–42 nm min⁻¹ temperature below 130 °C

to achieve a thickness of 200 nm, sufficient for a wide class of device requirements.

Acknowledgments

The authors would like to thank Professor Angus Rockett of the Department of Materials Science and Engineering, University of Illinois at Urbana-Champaign, for providing the prototype vacuum system and the SBIR (Small Business Innovation Research) program for the funding support through the administration of the US National Science Foundation (NSF). Materials characterization was carried out in part in the Frederick Seitz Materials Research Laboratory Central Facilities, University of Illinois, which are partially supported by the US Department of Energy under grants DE -FG02-07ER46453 and DE-FG02-07ER46471.

References

- [1] Berg S and Nyberg T 2005 *Thin Solid Films* **476** 215
- [2] Li N, Allain J P and Ruzic D N 2002 *Surf. Coat. Technol.* **149** 161
- [3] Matthews A 2003 *J. Vac. Sci. Technol. A* **21** S224
- [4] Gibson D R, Brinkley I, Wadell E M and Walls J M 2008 *Proc. SPIE* **7101** 710108
- [5] Laux S, Kaiser N, Zoller A, Gotzelmann R, Lauth H and Bernitzki H 1998 *Thin Solid Films* **335** 1
- [6] Liu C, Matsutani T, Asanuma T, Kiuchi M, Alves E and Reis M 2003 *Nucl. Instrum. Methods Phys. Res. B* **206** 348
- [7] Han Y, Kim D, Cho J S and Koh S K 2005 *Thin Solid Films* **473** 218
- [8] Kim D 2006 *Vacuum* **81** 279
- [9] Adurodija F O, Izumi H and Ishihara T 2000 *Vacuum* **59** 641
- [10] Kim D and Kim S 2002 *J. Vac. Sci. Technol. A* **20** 1314
- [11] Liao L S, Hung L S, Chan W C, Ding X M, Sham T K, Bello I, Lee C S and Lee S T 1999 *Appl. Phys. Lett.* **75** 1619
- [12] Minami T 2008 *Thin Solid Films* **516** 5822
- [13] Sudit I D and Chen F F 1994 *Plasma Sources Sci. Technol.* **3** 162
- [14] Ruzic D N 1994 *Electronic Probes for Low Temperature Plasmas (AVS Monograph Series)* ed W Weed (New York: American Vacuum Society Education Committee)
- [15] Green K M, Hayden D B, Juliano D R and Ruzic D N 1997 *Rev. Sci. Instrum.* **68** 4555
- [16] Kurdesau F, Khripunov G, da Cunha A F, Kaelin M and Tiwari A N 2006 *J. Non-Cryst. Solids* **352** 1466
- [17] Ray A, Banerjee R, Basu N, Batabyal A K and Barua A K 1983 *J. Appl. Phys.* **54** 3497
- [18] Kim Y S, Park Y C, Ansari S G, Lee J Y, Lee B S and Shin H S 2003 *Surf. Coat. Technol.* **173** 299
- [19] Bae J W, Kim H J, Kim J S, Lee N E and Yeom G Y 2000 *Vacuum* **56** 77
- [20] Luo S N, Kono A, Nouchi N and Shoji F 2006 *J. Appl. Phys.* **100** 113701
- [21] Lee W J 2002 *Solid State Electron.* **46** 477
- [22] Lee G H, Shin B C and Min B H 2002 *Mater. Sci. Eng. B* **95** 137
- [23] Mergel D, Stass W, Ehl G and Barthel D 2000 *J. Appl. Phys.* **88** 2437